Ultrasonics - Sonochemistry 45 (2018) 7–16

Contents lists available at ScienceDirect

Ultrasonics - Sonochemistry

journal homepage: www.elsevier.com/locate/ultson

Numerical modelling of acoustic pressure fields to optimize the ultrasonic cleaning technique for cylinders

Habiba Lais[a,b,*], Premesh S. Lowe[a], Tat-Hean Gan[a], Luiz C. Wrobel[b]

[a] Brunel Innovation Centre, Granta Park, Great Abington, Cambridge CB21 6AL, UK
[b] Brunel University, Kingston Lane, Uxbridge, Middlesex UB8 3PH, UK

ARTICLE INFO

Keywords:
Cavitation
COMSOL
Excitation
Fouling removal
Numerical modelling
Ultrasonic transducers

ABSTRACT

Fouling build up is a well-known problem in the offshore industry. Accumulation of fouling occurs in different structures, e.g. offshore pipes, ship hulls, floating production platforms. The type of fouling that accumulates is dependent on environmental conditions surrounding the structure itself. Current methods deployed for fouling removal span across hydraulic, chemical and manual, all sharing the common disadvantage of necessitating halting production for the cleaning process to commence. Conventionally, ultrasound is used in ultrasonic baths to clean a submerged component by the generation and implosion of cavitation bubbles on the fouled surface; this method is particularly used in Reverse Osmosis applications. However, this requires the submersion of the fouled structure and thus may require a halt to production. Large fouled structures such as pipelines may not be accommodated. The application of high power ultrasonics is proposed in this work as a means to remove fouling on a structure whilst in operation. The work presented in this paper consists of the development of a finite element analysis model based on successful cleaning results from a pipe fouled with calcite on the inner pipe wall. A Polytec 3D Laser Doppler Vibrometer was used in this investigation to study the fouling removal process. Results show the potential of high power ultrasonics for fouling removal in pipe structures from the wave propagation across the structure under excitation, and are used to validate a COMSOL model to determine cleaning patterns based on pressure and displacement distributions for future transducer array design and optimization.

1. Introduction

Fouling formation is a major problem for the offshore industry [1]. It is an important factor contributing to the assessment of service lifetime and safety of marine facilities [2]. Consequently, large sums of money are spent in cleaning and preventative measures to maintain offshore structures in a state of operation and efficiency. Current methods deployed for fouling removal include hydraulic, chemical and manual, having a common disadvantage – in that it is mandatory to halt the operation of the structure in order to commence the fouling removal process. Most common fouling mechanisms in offshore structures are; deposition of hard scale and the settlement and growth of marine organisms. This accumulation of fouling can occur in different engineering structures such as pipes and ship hulls. The type of fouling that can be accumulated is dependent on environmental conditions surrounding the structure itself.

Scaling occurs when saturated brine undergoes a temperature or pressure change causing the solubility to decrease, which results in the precipitation of solid crystals. The Calcium Carbonate (calcite) composition in pipelines is an example of the most common scaling problem in offshore structures. Other common scales that form in offshore process lines are Barium Sulphate (barite), Strontium Sulphate and Magnesium Sulphate [3]. Sometimes scaling can develop rapidly causing complete pipe blockage within 24 h [4]. On a slower timescale, biofouling is the growth of marine organisms. This includes algae, micro and macro organisms [5]. On complex and large offshore structures, fouling may be insignificant in relation to the structure's weight but fouling on the internal surface of the pipe is a significant problem when it causes blockages, rupture and damages to the structure.

The current removal methods deployed in industry can be costly and time consuming due to halts in production. A successful method of fouling removal is the use of chemicals [6] as this achieves up to 100% de-fouling but with the downside of negative environmental impact due to the release of chemicals after use, as well as down-time of the facility. Another promising method of fouling removal that has recently surfaced is the use of ultrasound. Currently, ultrasonic baths are used for cleaning individual parts of the offshore plant by generating cavitation bubbles which implode on the fouled surface [7,8], particularly in

* Corresponding author at: Brunel Innovation Centre, Granta Park, Great Abington, Cambridge CB21 6AL, UK.
E-mail addresses: habiba.lais@brunel.ac.uk (H. Lais), Tat-Hean.Gan@brunel.ac.uk, BIC@brunel.ac.uk (T.-H. Gan).

https://doi.org/10.1016/j.ultsonch.2018.02.045
Received 1 October 2017; Received in revised form 9 February 2018; Accepted 26 February 2018
Available online 03 March 2018
1350-4177/

Reverse Osmosis applications [9–11]. Conventionally, components that have accumulated fouling are submerged into an ultrasonic bath which yet again, requires stopping operation of the structure for the fouling removal process to commence.

The present paper investigates the potential of using High Power Ultrasonic Transducers (HPUT) to mimic the environmental condition of an ultrasonic bath in the pipe structures under investigation. The investigation is applied to a Stainless Steel 315 L pipe which is 300 mm in length, 1.5 mm in wall thickness and 50.08 mm in outer diameter with a thin layer of Calcite on the inner pipe wall. The paper is organized as follows. Theoretical background is given in Section 2 while Section 3 consists of the laboratory experimental setup followed by the Finite Element Analysis (FEA) in Section 4. Experimental and numerical results are discussed in Section 5 followed by discussions in Section 6, conclusions in Section 7 and finally, further work is suggested in Section 8.

2. Theoretical background

2.1. Ultrasonic cavitation

The fouling removal mechanism for the technique discussed in this work is by the development and implosion of acoustic cavitation bubbles. Acoustic cavitation can be defined as the formation of vapour bubbles due to a sudden decrease in pressure in a liquid caused by a (de-)compressional wave [12]. A rarefaction instant is thereby introduced and forms a vacuum, where a bubble can appear as shown in Fig. 1. During the oscillation of the bubble, the radius increases in the rarefaction instants and decreases in the compressional instants. In one of these cycles, the compression can burst the bubble (adiabatically) to produce pressures of up to 500 Bar and temperatures up to 5000 K.

There are two types of cavitation bubbles that can form within a liquid; stable cavitation where the bubbles oscillate for a long period of time in a sound field with a large number of cycles, and transient cavitation which lasts for less than one cycle and is violent enough to potentially damage the surface of the body in contact with the liquid [12]. Fig. 1 [13] illustrates and compares the development of stable and transient cavitation bubbles.

Due to stable cavitation bubbles oscillating for a period of time, they do not produce any light emission or chemical reactions when imploding. However, transient cavitation bubbles implode with a strong collapse, creating light emissions and/or chemical reactions within the liquid as a result of the implosion [14].

Although two types of cavitation have been defined, cavitation bubbles can also be a combination of both stable and transient cavitation, as discussed in the literature by Yasui in 2018 [14]. This phenomenon is also known as 'high energy stable' and 'repetitive transient cavitation'. Cavitation bubbles that are a combination of both types of cavitation oscillate for a long period of time similarly to stable cavitation however, they produce small amounts of light emission and chemical reactions. An example of this combination of both stable and transient cavitation can be found in Single-Bubble Sonoluminescence (SBSL) [15].

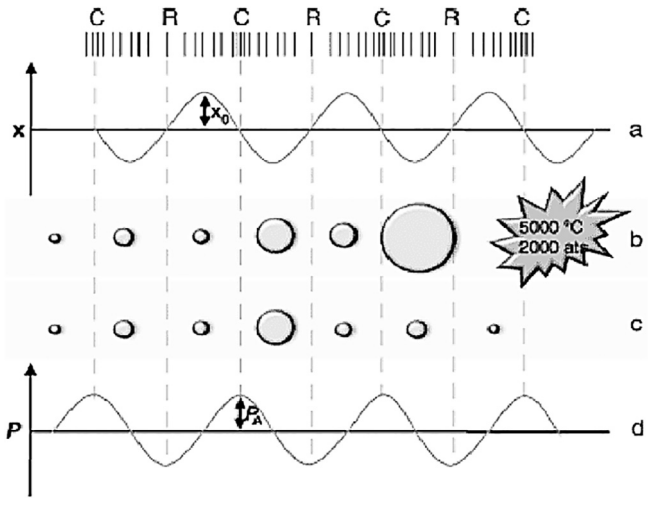

Fig. 1. Growth of stable and transient cavitation bubbles illustrating (a) displacement, (b) transient cavitation, (c) stable cavitation and (d) pressure [13].

Stable cavitation oscillates at the excitation frequency of the transducer as well as the harmonics and subharmonics of the cavitation [16]. These harmonics and subharmonics produce acoustic emission which can be detected to indicate the generation of the cavitation. The non-linear nature of a single spherical oscillating cavitation bubble is explained by the Rayleigh-Plesset equation [17]:

$$\frac{p(t)-p_{\infty}(t)}{\rho_L} = R\frac{d^2R}{dt^2} + \frac{3}{2}\left(\frac{dR}{dt}\right)^2 + \frac{4\nu_L}{R}\frac{dR}{dt} + \frac{2s}{\rho_L R} \quad (1)$$

where, $p(t)$ is the pressure within the bubble, assumed to be uniform, $p_{\infty}(t)$ is the external pressure infinitely far from the bubble, ρ_L is the density of the surrounding liquid, assumed to be constant, $R(t)$ is the radius of the bubble, ν_L is the kinematic viscosity of the surrounding liquid, assumed to be constant. S is the surface tension of the bubble.

2.2. Fouling removal

Ultrasound has been used for different applications such as welding, stimulation of chemical activity, sonochemical destruction of living cells, crystallization, chemical activation and cleaning [18,19]. The acoustic cavitation phenomenon is used in ultrasonic cleaning applications. The acoustic cavitation bubbles are generated due to the high pressure vibration generated by Langevin bolt clamped HPUTs [20]. These transducers generate ultrasonic compressional waves which can travel through a liquid and generate cavitation if the transducer is exciting at its main resonant frequency and achieving the required pressure amplitude to surpass the cavitation threshold.

Applications of cleaning using ultrasonics, specifically ultrasonic baths, have been implemented to assist the cleaning of membranes for ultrafiltration. HPUTs have been used in various applications such as removing juvenile barnacles [21], removing pesticides on strawberries without damaging the strawberries [22], cleaning 3D printed parts using a dissolution liquid with ultrasonic cavitation [23], assisting fish reproduction studies by separating the oocytes from each other and from the ovarian tissue [24] and ultrasonically cleaning turbine engines' oil filters [25].

An example of a membrane cleaning application is for controlling fouling formation in membrane ultrafiltration of waste water [26]. The studies showed that ultrasound-assisted cleaning reduces the membrane fouling. They also showed a relationship between the frequency applied (when exciting at a low frequency ~35 kHz), and the slowdown of the fouling formation. Exciting at higher frequencies (~130 kHz), leads to improved fouling removal. The results showed better cleaning at the location of radicals within the bulk liquid attributed to exciting at a higher frequency [26].

Furthermore, research has been carried out on applying the ultrasonic technique to heat exchangers [27]. It has been shown that the fouling removal patterns match the locations of nodes and antinodes at the start of cleaning, and, in time, expands along the vibrating length.

The four anti-fouling mechanisms known as Acoustic Streaming, Micro Streaming, Micro Jets and Micro Streamers have been discussed in the literature [28] and are the physical effects produced from ultrasonic cavitation. The mechanisms driven by cavitation were applied to different applications for cleaning, particularly in biofouling removal. Exciting at low ultrasonic frequencies such as 20 kHz created strong shear forces resulting in the four anti-fouling mechanisms to be

created from the ultrasonic cavitation.

2.3. Finite element modelling (FEM)

Literature gives various methods to model the generation of cavitation. However, each model is limited to modelling a small number of cavitation bubbles due to the complexity of this phenomenon [29–31]. Another approach to model ultrasonic cleaning is by mapping the pressure distribution and correlate this to the potential for cavitation on reaching the pressure threshold required for cavitation to be generated.

A study which modelled the prediction of ultrasonic cleaning was conducted by Lewis et al. [32] who correlated the cavitation pressure threshold found from experiments with the computed pressure distribution to predict the emergence of cavitation at pressure locations above the threshold. The work stated that the minimum pressure required for cavitation to occur in water is 5 Bar [33] and requires a pressure amplitude large enough to overcome the tensile stress bonds [34]. This work shows the potential to create a simplified model for predicting cleaning from the pressure distribution.

Although the initial pressure required for generating cavitation can be modelled, this neglects the effect from cavitation generation which can in fact change the pressure distribution across the fluid medium [35].

The equation used to calculate the solid line in Fig. 2 is the spatial distribution of the pressure amplitude:

$$p_a(x) = \rho c v_0 \left| 2\sin\left(\frac{\pi}{\lambda}\sqrt{x^2 + a^2} - x\right)\right| \quad (2)$$

where $p_a(x)$ is the acoustic pressure amplitude at position x, x is the distance from the circular piston on the symmetry axis, ρ is the liquid density, c is the sound velocity in the liquid, v_0 is the velocity amplitude of the horn tip, λ is the wavelength of ultrasound within the liquid, a is the radius of the circular piston.

Yasui et al. [35] discusses the change in acoustic amplitude when cavitation is being generated to be a third of the pressure produced in a fluid medium producing no cavitation. This shows the ratio of cavitation generated fluid to be a third of the fluid with no cavitation. When applying this ratio to an FEA model which neglects cavitation generation, the pressure distribution will over estimate values to be 3 times larger.

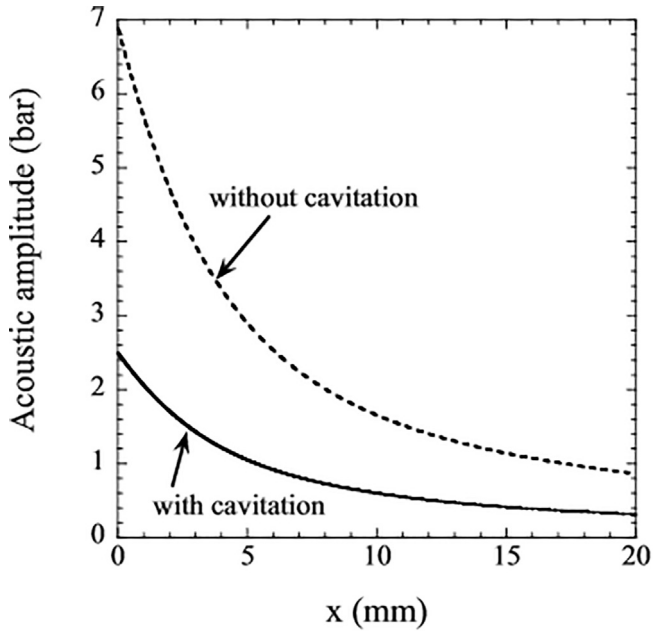

Fig. 2. Calculated acoustic amplitude under an ultrasonic horn as a function of the distance from the horn tip on the symmetry axis. The dotted curve is the calculated result (experimental) by Eq. (2). The solid curve is the estimated one by the comparison of the numerical simulation and the experimental observation [34].

Moholkar et al. in 2000 [33] stated a minimum of 5 Bar to generate cavitation but as this model neglected cavitation, they also did not consider that the presence of cavitation will affect the pressure distribution. Also, the minimum pressure required to generate cavitation is uncertain as the recent work by Yasui in 2018 [14] stated that a 40 kHz resonant transducer required approximately 1–2 Bar of pressure as the minimum cavitation threshold.

The generation of cavitation within a fluid reduces the pressure amplitude within the acoustic field, thus attenuating the acoustic wave into the surrounding liquid [36]. Due to the ultrasonic wave being applied onto the wall of a structure, this vibrates the wall due to the pressure oscillation. The strong vibration of the wall radiates strong acoustic waves. But also, the acoustic field depends on the material of the wall and the attenuation coefficient of the ultrasound (which increases with the addition of cavitation bubbles). The increase in attenuation decreases the wall vibration. Another effect on the acoustic field which requires further research is the degassing of bubbles within the fluid [36].

As this paper focuses on the vibration of the cylindrical specimen to produce cavitation, the radiation of the wall must be considered. Yasui et al. [37] describe the importance of coupling the radiation of the reactors wall within the sonochemical reactor. They have described literature where the vibration of the wall has been neglected in several pieces of research, however, research papers that have included the effects of the vibration of the wall by coupling this interface with the fluid domain but neglected the effects of cavitation bubbles within the sonochemical reactor. Yasui et al. [35] implemented numerical simulations which couple the vibration of the wall of the sonochemical reactor but also take cavitation bubbles into account by changing the attenuation coefficient of the model due to the relationship between attenuation and cavitation bubbles. Cavitation bubbles not only affect the attenuation on the vibration wall but also the speed of sound within the fluid domain, but this effect was neglected in Yasui et al. [35] and the speed of sound of the liquid kept constant.

In recent years, the use of the COMSOL Multiphysics package has become popular for modelling cavitation bubbles and for mapping the pressure distribution [38]. COMSOL allows the incorporation of different physical effects related to cavitation generation and ultrasonic cleaning. The approach can be adopted to neglect the development of cavitation bubbles and focus solely on the pressure distribution, to assist in designing ultrasonic cleaning systems [38,39].

3. Experimental set-up

The purpose of the experimental set-up is to demonstrate the fouling removal capability using ultrasonic [40]. The fouled sample undergoes localized ultrasonic cleaning for comparison with the COMSOL model.

The fouling within the pipe is generated in advance using electrochemical reactions to create a crystallization fouling known as Calcite [40]. Fig. 3 shows the pipe sample immersed in a Calcium Carbonate solution where the electrochemical reactions, electrolysis and hydrolysis take place rapidly, depositing calcite on the inner wall of the pipe.

3.1. Transducer modification and attachment

The transducer used for this technique has undergone machining of the contact surface to increase the contact between the transducer and pipe specimen (Fig. 4). This modification allows a larger surface of the pipe to undergo high pressure amplitude for cavitation to be generated.

A transducer holder with a ratchet strap is used to hold the transducer in place and acoustic coupling gel is applied on the contact surface of the transducer before attaching to the pipe to ensure that there are no trapped air bubbles between the transducer and pipe in order to maintain a rigid contact.

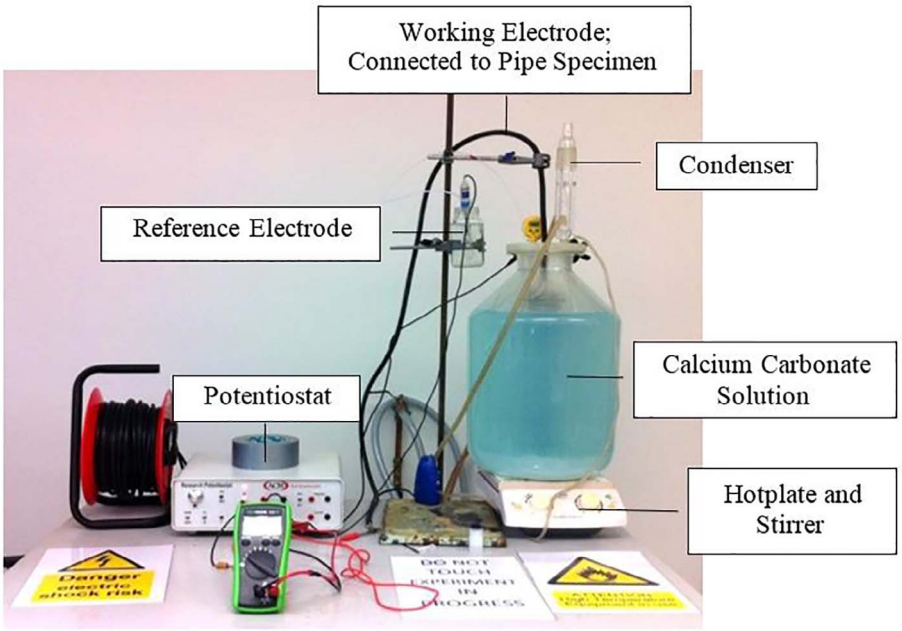

Fig. 3. Preparation of fouled sample (calcite) in laboratory conditions, illustrating the fundamental equipment used to generate electrochemical reactions. This sample is used for experimental validation. Sample used was a 300 mm length, 1.5 mm wall thickness, 50.08 mm outer wall diameter stainless steel pipe.

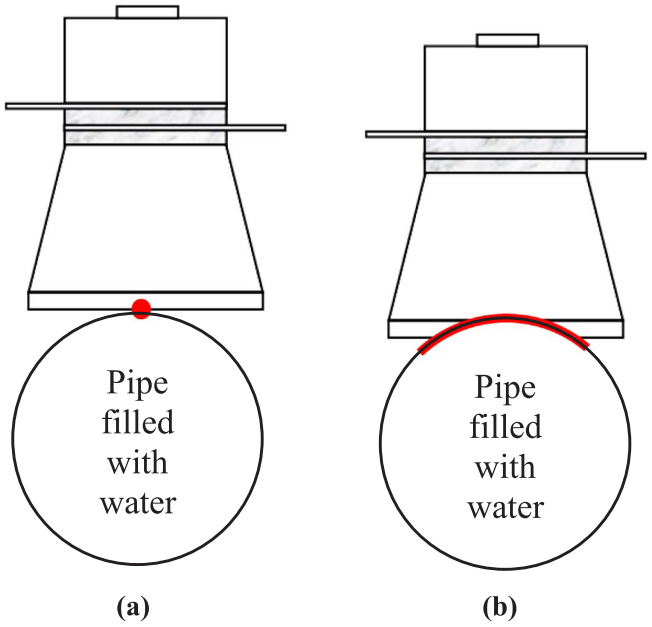

Fig. 4. Illustration of (a) standard transducer and (b) concave transducers used to achieve better contact onto pipe.

3.2. Fouling removal set-up

The experimental set-up for fouling removal includes a signal generator and power amplifier for transducer excitation. The 3D Laser Doppler Vibrometer (3D-LDV) was used for data acquisition (Fig. 5).

The fouling removal experiment includes the following list of equipment:

- Acoustic Coupling Gel
- Transducer Holder with ratchet strap
- Concave 40 kHz Langevin Transducers
- Polytec PSV-500 3D-LDV
- 1040L Power Amplifier
- DSO-X 2012A Oscilloscope
- Stainless Steel 315 L Pipe – 300 mm length, 1.5 mm wall thickness, 50.08 mm outer wall diameter with calcite on inner wall

The sinusoidal wave input signal is pulsed by a DSO-X 2012A Oscilloscope. The frequency is adjusted to the resonance value and remains constant throughout the experiment. The amplitude is adjusted to 1 V and sent to the 1040 L Power Amplifier.

The 1040 L Power Amplifier, covering the frequency spectrum of 10 kHz–5 MHz at 55 dB gain, sends the amplified signal to the transducer. The 40 kHz transducer is placed on a Stainless Steel 315 L pipe which is 300 mm in length, 1.5 mm in wall thickness and 50.08 mm in outer diameter with a thin layer of Calcite on the inner pipe wall.

During the fouling removal trials the Polytec 3D-LDV is used to measure the vibrations of the structure undergoing wave propagation from the transducer. The 3D-LDV was used in previous studies to investigate the ultrasonic stress distribution on a pipe surface [41]. The displacement on the outer surface can be compared with cleaning patterns to match the nodes and antinodes on the outer surface with the cleaning patches found on the inner wall.

4. FEA theory and methodology

To assist with understanding how wave propagation can promote larger coverage of fouling removal over a structure, an FEA model was created in COMSOL Multiphysics 5.2a. The model consists of a Langevin transducer placed on a stainless steel pipe, matching the dimensions and material properties of the experimental specimen. The components for a Langevin transducer are as follows and shown in Fig. 6.

- PZT Ceramic rings (compressional) – 1/8 wavelength
- Two contact plates
- Front mass – 1/2 wavelength length
- Back mass
- Bias bolt with nut – 1/4 wavelength length
- Epoxy resin - as adhesive and acoustic couplant between components

The model neglects the contact plates and epoxy resin within the

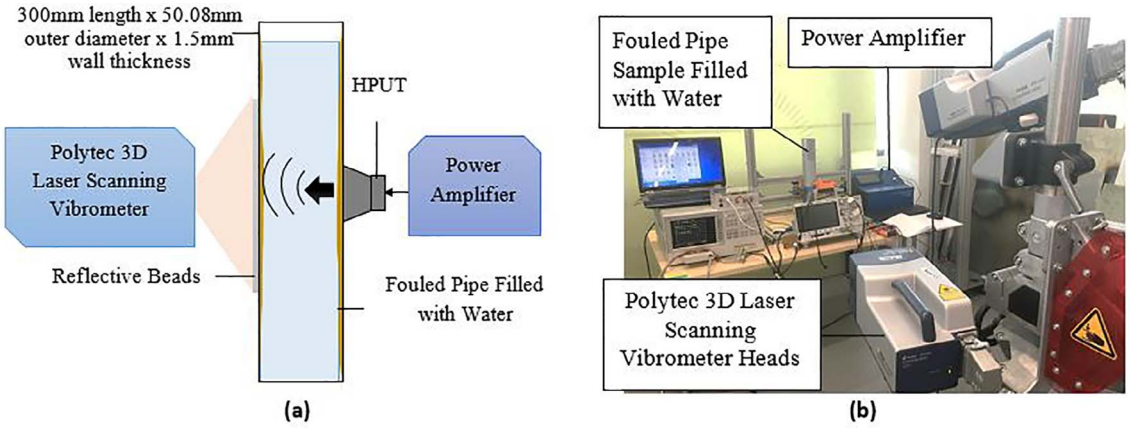

Fig. 5. (a) Schematic of fouling removal experimental set-up and (b) photograph of experimental set-up showing the use of 3D-LDV to capture surface displacement to compare with numerical results.

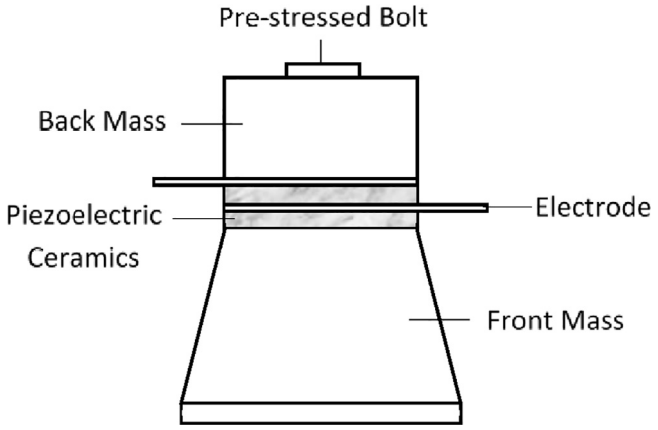

Fig. 6. Illustration of main components of HPUT.

transducer. Instead, the voltage is applied directly to the faces of the piezoelectric ceramic rings.

Several COMSOL physics modules are incorporated into the model to account for the transducer excitation through the solid pipe wall and into the fluid domain. The specific physics used are as follows:

- Pressure Acoustics, Transient
- Electrostatics
- Solid Mechanics
- Piezoelectric Effect
- Acoustic-Structure Boundary

4.1. Numerical simulation

For the Pressure Acoustics, this is assigned to the fluid domain and uses the wave equation:

$$\frac{1}{\rho c^2}\frac{\partial^2 p_t}{\partial t^2} + \nabla\cdot\left(-\frac{1}{\rho}(\nabla p_t - q_d)\right) = Q_m \tag{3}$$

where, ρ is the total density, p_t is the total pressure, ρc^2 is the bulk modulus, q_d is the dipole source and Q_m is the monopole source.

The monopole source can be found using the following equation:

$$|p(r)| = i\rho c\frac{Qk}{4\pi r} \tag{4}$$

where, p is the pressure amplitude, r is the distance, ρ is the density of water, c is the speed of sound, Q is the source strength, k is the wave number.

The dipole source is found using the following equation:

$$|p(r)| = \left|-i\rho c\frac{Qk^2 d}{4\pi r}\cos\theta\right| \tag{5}$$

where, d is the horizontal distance between two sources and θ is the angle between them.

The sound pressure level settings use the reference pressure for the selected fluid. The model is also set to atmospheric pressure and temperature. The transient pressure acoustic model is set to be *linear elastic* and exhibits the speed of sound and density from the material assigned to the fluid domain. The fluid has linear elastic behavior governed by Newton's second law while solid mechanics physics is applied to the rest of the model as these components are solid. The physics is governed by the Navier equation:

$$\rho\frac{\partial^2 u}{\partial t^2} = \nabla\cdot FS + F_V \tag{6}$$

where, ρ is the fluid density, u is the velocity of the fluid, F is the deformation gradient, F_v is a body force, S is the second Piola-Kirchhoff stress tensor.

All solid parts excluding the piezoelectric ceramic rings will obey their material properties and are considered to be of linear elastic material. Piezoelectric material is assigned to the piezoelectric ceramic rings which obey the solid mechanics governing equations and, additionally, the PZT- linearized constitutive equations in stress-charge form:

$$T = c_E\cdot S - e^t\cdot E \tag{7}$$

$$D = e\cdot S + \varepsilon_S\cdot E \tag{8}$$

where, T is the tensor stress field, S is the strain field, E is the electrical field component, D is the electric displacement field, c_E is the elasticity matrix, e is the piezoelectric coupling coefficient for the stress-charge form, ε_S is the permittivity matrix. The subscripts E and S denote constant electric field and strain, respectively.

Electrostatic phenomena are included only in the piezoelectric ceramic rings where the signal is applied using the following formula:

$$\nabla\cdot D = \rho_V \tag{9}$$

$$E = -\nabla V \tag{10}$$

where, $\nabla\cdot D$ is the electric charge density, ρ_V is the electric charge concentration and E is the electric field due to the electric potential V.

The terminal and ground equipotential are applied to the boundaries explicitly as previously specified. The ground boundary is set equal to 0 V and the terminal boundary is set to:

$$V = V_0 \tag{11}$$

where, *Vo* is the modulating 40 kHz, 500 Vpk-pk sine waveform to replicate the signal generated in the experimental setup as explained in

Section 3. Correct polarization is achieved by assigning a rotated global co-ordinate system to change the direction of polarization of one of the piezoelectric ceramic rings.

Multiphysics modules are assigned to couple the pressure acoustics and solid mechanics physics across the acoustic-structure boundary between the fluid and solid domain. This allows the radiation of the wall due to transducer excitation to be taken into account and create high and low pressure to propagate into the fluid domain [37]. For this reason, COMSOL is used to incorporate required physics to simulate the experimental configuration for the present study.

In the experiment, the coupling of the transducer contact surface to the pipe surface is done by applying acoustic couplant gel between the contact surface of the transducer and pipe to remove any air bubbles which can affect the ultrasonication performance. The COMSOL model mimics this attachment by using integration on the boundary between the transducers contact surface and pipe surface. A fixed constraint is placed on the top of the transducer and the transducer holder is ignored within the model.

As this model neglects the presence of cavitation bubbles, the resulting attenuation and acoustic radiation affects are not considered [36] however, some attenuation has been applied to his model by altering the bulk viscosity of the fluid domain.

The effects of decreased radiation from the presence of cavitation has been discussed in Section 2 [35] and has not been taken into account in the model methodology. As this model is not considering the effects of cavitation decreasing the sound velocity and acoustic field which is caused by the presence of cavitation.

4.2. Meshing

A dynamic transient simulation to map out the propagation of the wave requires the calculated mesh to be optimal. The wave equation requires the time stepping within the solver to complement the meshing itself to yield an accurate solution. The meshing size requires five 2nd-order mesh elements per wavelength. The equation used to calculate the maximum allowed mesh element size (*ho*) [42] is given by:

$$h_o = \frac{c}{Nf_o} \tag{12}$$

where, c is the velocity, N is number of elements per wavelength and f_o is the center frequency.

Free Tetrahedral elements are used for a high density around the transducer location, the remainder of the geometry is swept as follow (13),

$$Sweep\ density = \frac{2800mm}{h_o} \tag{13}$$

The selected study for this model is *Transient*, so that the simulation can generate results as the modulated sine wave propagates from the transducer.

The increments are based on the maximum allowed mesh element size. The time steps are chosen to resolve the wave equally over time whilst the meshing is placed to resolve the wave propagation over the model itself. Time steps must be optimized relative to the mesh and this is supported with the relationship between mesh size h_o and time step (Δt):

$$t_x = \frac{c\Delta t}{h_o} \tag{14}$$

The t_x ratio is given as 0.2 as it is suggested to be near optimal and by rearranging the Eq. (14), the time steps are calculated using (15):

$$\Delta t = \frac{t_x h_o}{c} = \frac{0.2h_o}{c} \tag{15}$$

Table 1
parameters of HPUT used for the fouling removal experiment.

Parameter	Value
Transducer Power	40 W
Transducer Resonant Frequency	40 kHz
Transducer Material	Stainless Steel
Power Input	65 W
Excitation Frequency	40.46 kHz

5. Results and analysis

The fouling removal experiment examines a stainless steel pipe with a thin layer of calcite on the inner wall. The excitation from a HPUT was used to clean an area of the calcite from the inner pipe wall whilst measuring outer wall displacements using the 3D-LDV. Vibrometry analysis shows high displacement at the locations of fouling removal of the pipe sample.

The parameters of the experiment and achieved displacements according to the Vibrometry data are summarized in Table 1. These experimental values are replicated in the COMSOL model.

The modelled pipe specimen is a Stainless Steel 315 L pipe which is 300 mm in length, 1.5 mm in wall thickness and 50.08 mm in outer diameter. The model assumes two lines of symmetry as shown in Fig. 7. A single quadrant of the pipe is modelled to reduce the computation size.

5.1. Pipe displacement contours

To validate the model, the predicted pipe displacement is compared with the Vibrometry results. Fig. 8 shows the comparison of the cleaned area with Vibrometry scan and COMSOL model. Each set of results show an overlap of high displacement where cleaning results were achieved. With the variables from Table 1, the developed model shows a good agreement between high displacements and cleaning patterns. The model results in Fig. 8 shows high displacements propagating from the transducer and localized at the circumference of the pipe perpendicular to the transducer attachment. The direction of propagation is

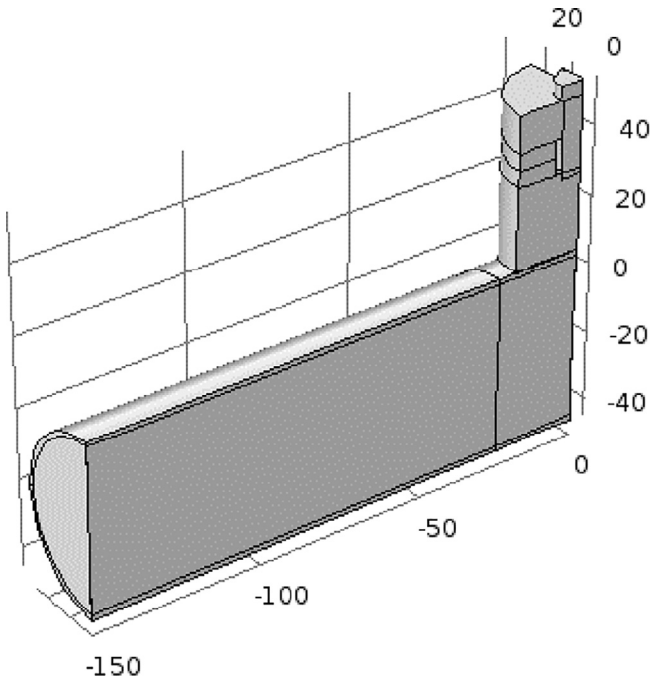

Fig. 7. Geometry of COMSOL model displaying cut planes at lines of symmetry for computation efficiency.

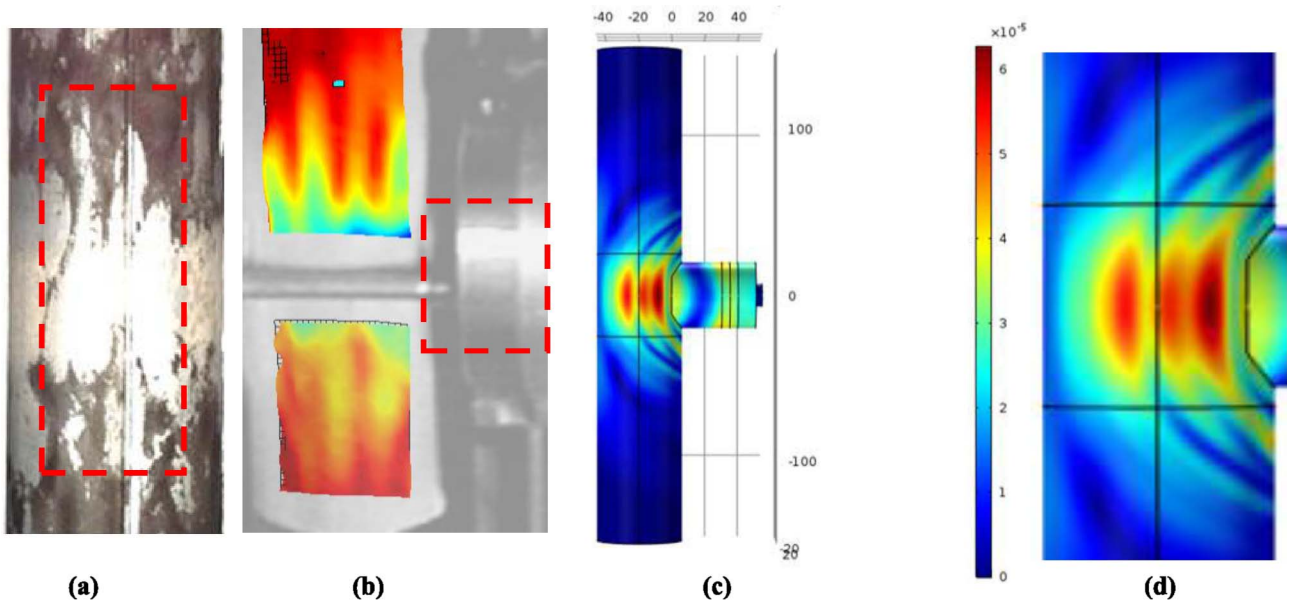

Fig. 8. Comparison of results (a) experimentally obtained localized cleaning after one cycle of ultrasonic cleaning, (b) 3D displacement measured during ultrasonic cleaning using 3D-LDV, (c) numerical simulation results and (d) zoomed version of (c) displaying high displacement achieved at same location of cleaning and 3D-LDV results.

due to the transducer producing compressional waves.

5.2. Acoustic pressure contours

As the model validates the cleaning patterns, the next step is to validate whether an arbitrary experimental set-up is generating cavitation bubbles prior to undergoing experiments using the pressure threshold. Since this set-up has shown to achieve cavitation generation for the cleaning results to be obtained, the COMSOL model is assumed to be generating cavitation.

The total acoustic pressure is shown in Fig. 9 for the same time instant as in Fig. 8, as stated previously, a minimum of 1–2 Bar must be applied by the transducer to create acoustic cavitation [14]. The results show the surface of the transducer to have achieved a pressure value above 5 Bar, thus meeting the requirement for producing acoustic cavitation. The pressure then propagates in the liquid and spans the location of cleaning.

As the pressure continues propagating throughout the liquid, instants of high positive and negative pressure are in-lined with the cleaning pattern. The negative pressure instants can be linked to the rarefactions within the liquid where cavitation bubbles are generated and the positive pressure instants relate to the compressional locations in which the generated bubbles implode.

Fig. 9 displays the isosurface plot of the total acoustic pressure for the time steps discussed at the cross section of the symmetry planes to expose the pressure contours within the fluid domain. The transducer location shows a pressure of 7 bar which is above the pressure required for cavitation. This location is assumed to be generating the compressional instant of the high pressure wave. Travelling through the fluid, there is a high (peak) pressure drop to -7 Bar which represents the rarefaction instants, where cavitation bubbles appear.

5.3. Fast Fourier Transform

A Fast Fourier Transform (FFT) is carried out on the 3D-LDV results. Fig. 10 shows the average velocity magnitude across the scanned points at different frequencies. The FFT displays a similar correlation between the average magnitude of velocity in the x, y and z directions. There is a significant peak in velocity at 40 kHz due to the resonance of the transducer and excitation frequency. This peak is followed by a harmonic at 80 kHz.

Peak values in the FFT graph from the Vibrometry results are due to the shockwaves emitted from the violent collapse of the cavitation bubbles generated within the fluid of the pipe specimen [43]. Each peak can be calculated based on the operating frequency, f_o.

$$f_o = 40kHz \tag{16}$$

$$Harmonics = nf_o \tag{17}$$

where, n is the natural number. For example, if n equals 1, 2, 3, 4, then the harmonics would be at 40, 80, 120 and 160 kHz respectively.

$$Half\ order\ subharmonic = \frac{f_o}{2} = 20kHz \tag{18}$$

$$ultraharmonics = \frac{(2n+1)f_o}{2} \tag{19}$$

$$If\ n = 1 \rightarrow \frac{3f_o}{2} = 60kHz$$

The calculated peaks produced from shockwave emissions has a good agreement with the peaks found in Fig. 10. When zooming into the 40 kHz peak, there is a large peak in velocity in the z-direction due to the high out-of-plane vibration, which is the vibration mechanism required for cleaning results to be achieved.

The COMSOL results were converted using FFT for ease of comparison with the Vibrometry results. A single point is selected on the pipe surface to plot the out-of-plane displacement *versus* frequency. Fig. 11 shows a significant peak at 40 kHz, matching the vibrometry results illustrated in Fig. 10. Overall there is a good agreement between numerical and experimental results of the consonant frequency for the investigated conditions.

Another clear comparison made from both Figs. 10 and 11 is between the various peaks that follow the resonant harmonic in the Vibrometry results that do not appear in the COMSOL model results. The reason for this is that the Vibrometry analysis is obtaining data from a specimen which is undergoing cavitation generation within the liquid. The cavitation bubbles emit shockwaves which resulted in the vibration of the pipe wall at frequencies other than the operating frequency. The COMSOL model neglects the generation of cavitation bubbles which means that there are no shockwaves being generated due to cavitation and result in frequency peaks other than at the resonance frequency.

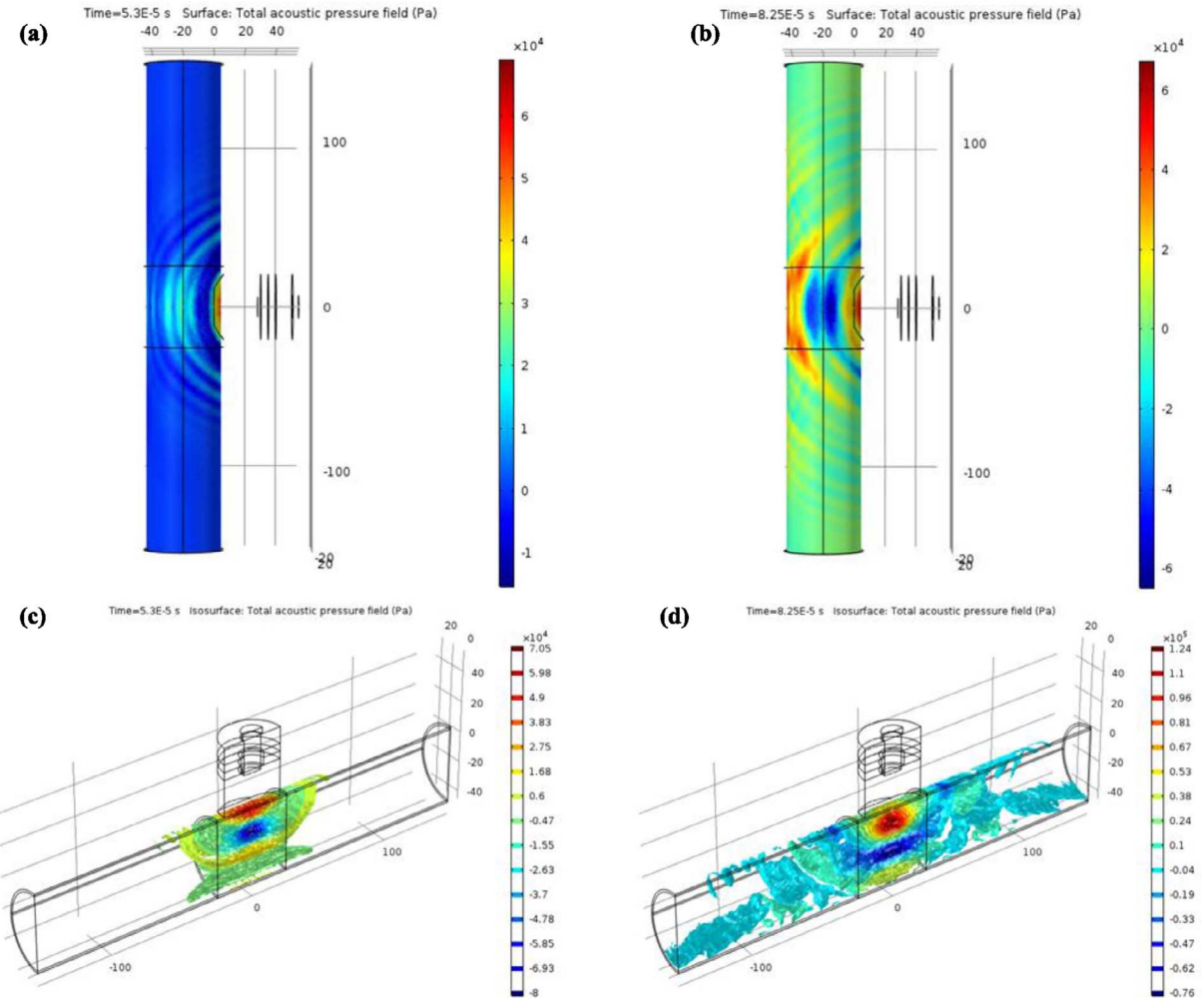

Fig. 9. Numerical results displaying acoustic pressure of pipe filled with water at (a) 530 ms and (b) 825 ms and the isosurface plot of acoustic pressure at (c) 530 ms and (d) 825 ms.

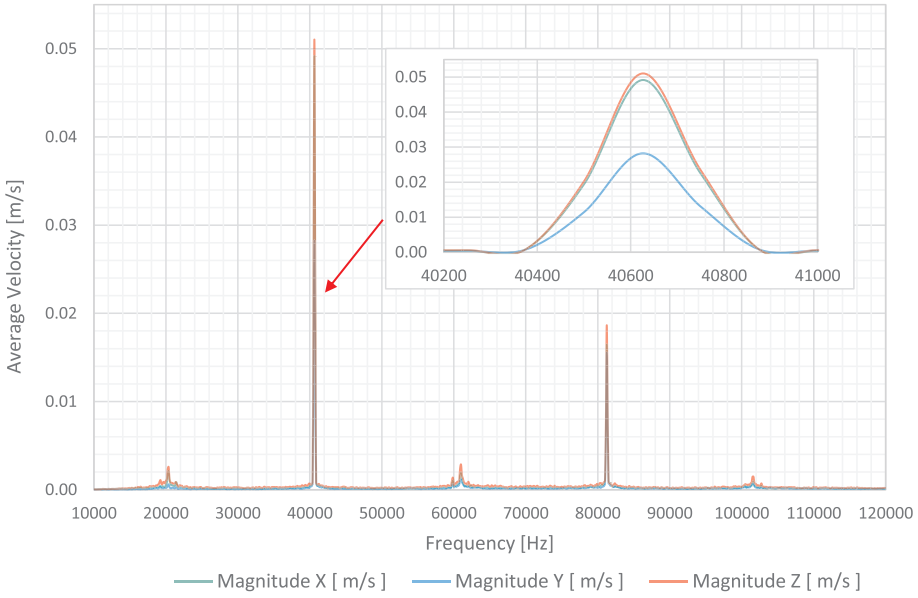

Fig. 10. FFT of average velocity of scanned area using 3D-LDV measurements taken of 40 kHz HPUT attached to pipe geometry illustrated in Fig. 5.

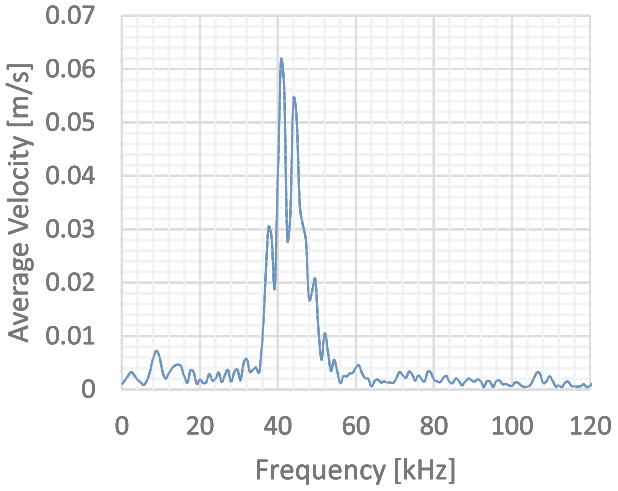

Fig. 11. FFT of numerical results obtained from single point on outer pipe surface, displaying the average velocity.

6. Discussions

6.1. Power requirements

The energy requirement depends on the application. The power requirement for intense cleaning applications is in the range of 70–100 W and the application in the current study requires 40–70 W to achieve an adequate level of cleaning. The transducers used in this study operates at 40 W and the input power of 65 W was required to compensate for power loss. The power requirement can be calculated as follow:

$$Average\ Watts\ Power = \frac{\pi r^2 h}{231} 100 \tag{20}$$

where, r is the radius of the inner pipe wall and h is the length of the pipe.

When attaching a transducer onto a structure, this affects the initial impedance of the transducer which shifts to a higher impedance value. The change in impedance will affect the required input power to achieve 250 V AC. The cleaning cycle time used for the experimental validation was 30 min. The calculation of the energy required for cleaning uses the following equations:

$$E_{(J)} = P_W \times t_s \tag{21}$$

where, E is the energy, P_w is the power and t_s is the duration of cleaning.

6.2. Transducer configuration

The transducer configuration used in the present study gives confidence to predict the cleaning patterns achieved from a transducer configuration on a fouled specimen. Further investigation must be carried out using the FEA model to analyze different configurations with the prospects of fouling removal over longer distances. The proposed model can help to select an optimized configuration to demonstrate its cleaning capabilities in laboratory conditions before using the method to predict cleaning on other fouled samples. Potential configurations include using an array of transducers over a large length or circumference.

6.3. Transducer attachment

The attachment and detachment of the transducers from the pipe specimen is crucial for this technique to be applied for commercial use. The method discussed in this study uses a transducer holder which straps the transducer onto the pipe and is tightened to 5 Bar of pressure whilst ensuring acoustic coupling gel is applied between the transducer contact surface and pipe. This method allows the strap to slide over the pipe for experimental purposes.

For commercial use, a more universal and user-friendly method must be designed to allow the holder to wrap over the circumference of a pipe without sliding through an open end of a pipe. Also, this method should accommodate the potential of requiring multiple transducers over a circumferential area resulting in linkages between multiple transducers and transducer holders to cover the pipe as required. To control the initial pressure applied onto the transducer via the holder, this can be measured using a thin film flexible pressure sensor which can be embedded into the power electronics and monitor the pressure applied, easing the attachment for the user.

7. Conclusions

This work uses a non-invasive method of fouling removal using power ultrasonics. The technique itself is carried out by using tailored bespoke HPUTs which are attached directly to the outer wall of the structure (submerged/filled with liquid) of interest. The excitation of the transducer is at its known natural resonant frequency and results in cavitation bubbles generated within the liquid. The implosion of these bubbles occurs on the fouled surface resulting in forces large enough to remove the fouling. Out-of-plane vibration of the structure itself due to (direct) transducer excitation also contributes to fouling removal, particularly at the location of transducer attachment, resulting in localized cleaning.

The work describes the experimental set-up which uses a 3D-LDV to acquire the out-of-plane displacements of the fouled pipe sample under investigation. The parameters for successful fouling removal during the experimental trials were compiled and used as inputs to the numerical model. The COMSOL model is based on the experimental set-up including the transducer, pipe and water but neglects the calcite layer and the mechanism for generation of cavitation. As the model only focuses on the pressure distribution and solid displacement, these are compared with the Vibrometry data and with the pressure thresholds for cavitation stated in the literature.

The results show a promising comparison of the displacement of the pipe between the COMSOL model and the Vibrometry results. These high nodal displacements are concentrated in the same areas of the cleaning pattern. However, the displacement values obtained in COMSOL were greater than the Vibrometry results. This is likely to be caused by neglecting the Calcite layer in the COMSOL model. This will be quantified in further investigations.

The acoustic pressure field plotted in COMSOL is compared with the pressure threshold reference of 5 Bar to determine whether the model can confirm if exceeding the cavitation pressure threshold of 5 Bar is possible. The model showed both pressure increases (compressional instants) and decreases (rarefaction instants) as large as 5 Bar. This pressure profile initially begins at the transducer location and later, propagates across the area which had undergone successful cleaning. Such an experimentally validated numerical simulation is proposed to optimize the non-invasive ultrasonic cleaning procedure for future applications.

8. Further work

The COMSOL model neglected the calcite layer which may explain why it predicted larger displacement values compared to the Vibrometry results and will need to be investigated further to understand the effects of modelling calcite and other layers of fouling. This can also be explained by neglecting the presence of cavitation bubbles. Yasui [35] discusses how the pressure field without the presence of cavitation is much larger than with cavitation. The effects of pressure can be considered using Eq. (2) to obtain pressure and displacement

values that match more similarly to the experimental results.

In regards to the cleaning capabilities, there is potential for fouling removal using the ultrasonic cleaning technique demonstrated by the localized cleaning results. However, optimization is the next step to improve the coverage of cleaning which can be implemented using the proposed COMSOL model to determine the best array of transducers, frequency and other input parameters.

Further investigation on the technique itself are needed for improving its Technology Readiness Level (TRL). This includes investigating the effects of coupling between the transducer contact surface and the fouled specimen to measure the change in cleaning capabilities based on the use of acoustic coupling gel, dry contact and permanently bonding the transducer onto the specimen.

By identifying the key factors in ensuring maximum cleaning, the procedure for attaching/detaching transducers could be optimized for cleaning for commercial use and ease of use for the end user. Other suggested factors include modification of the transducer contact surface, configuration of multiple transducers, cabling and power electronics.

Acknowledgments

This investigation was conducted as part of Innovate UK projects CleanMine and HiTClean, grant numbers 101333 and 102491, respectively. The authors express deep gratitude to Ignacio Garcia de Carellan and Makis Livadas of Brunel University London for all their efforts and contributions to the projects and this work.

References

[1] A.S. Paipetis, T.E. Matikas, D.G. Aggelis, D. Van Hemelrijck, Emerging Technologies in Non-Destructive Testing V, [Imprint] CRC Press, 2012.
[2] T. Yan, W.X. Yan, Fouling of offshore structures in China-a review, Biofouling 19 (S1) (2003) 133–138.
[3] A.G. Pillai, A study on mitigating the effect of sulphates in lime stabilised Cochin marine clays, PhD Thesis Cochin University of Science & Technology, India, 2014.
[4] M. Crabtree, D. Eslinger, P. Fletcher, M. Miller, A. Johnson, G. King, Fighting scale—removal and prevention, Oilfield Rev. 11 (3) (1999) 30–45.
[5] D. Yebra, S. Rasmussen, C. Weinell, L. Pedersen, Marine fouling and corrosion protection for offshore ocean energy setups, 3rd Int Conf. Ocean Energy Bilbao, Spain, (2010).
[6] "Ocean Team Group as." [Online]. Available: http://www.oceanteam.eu/. [Accessed: 14-Mar-2017]
[7] "Hilsonic." [Online]. Available: http://www.hilsonic.co.uk/. [Accessed: 14-Aug-2017]
[8] "Ultrawave." [Online]. Available: http://www.ultrawave.co.uk/. [Accessed: 14-Aug-2017]
[9] H. Maddah, A. Chogle, Biofouling in reverse osmosis: phenomena, monitoring, controlling and remediation, Appl. Water Sci. (2016) 1–15.
[10] M.O. Lamminen, Ultrasonic Cleaning of Latex Particle Fouled Membranes, PhD Thesis Ohio State University, USA, 2004.
[11] H.-C. Flemming, Reverse osmosis membrane biofouling, Experim. Therm. Fluid Sci. 14 (4) (1997) 382–391.
[12] C.E. Brennen, Cavitation and Bubble Dynamics, Cambridge University Press, 2013.
[13] "Creation of stable and transient cavitation bubbles." [Online]. Available: https://www.hielscher.com/wp-content/uploads/stable-transient-cavitation-Santos-et-al.-2009-opt.png. [Accessed: 25-Jan-2018]
[14] K. Yasui, Acoustic Cavitation, Acoustic Cavitation and Bubble Dynamics, Springer, 2018, pp. 1–35.
[15] M.P. Brenner, S. Hilgenfeldt, D. Lohse, Single-bubble sonoluminescence, Rev. Modern Phys. 74 (2) (2002) 425.
[16] R. Esche, Untersuchung der schwingungskavitation in flüssigkeiten, Acta Acustica united with Acustica 2 (6) (1952) 208–218.
[17] M.S. Plesset, A. Prosperetti, Bubble dynamics and cavitation, Ann. Rev. Fluid Mech. 9 (1) (1977) 145–185.
[18] T. Mason, L. Paniwnyk, J. Lorimer, The uses of ultrasound in food technology, Ultrason. Sonochem. 3 (3) (1996) S253–S260.
[19] J.A. Gallego-Juarez, High-power ultrasonic processing: recent developments and prospective advances, Phys. Proc. 3 (1) (2010) 35–47.
[20] S. Lin, F. Zhang, Measurement of ultrasonic power and electro-acoustic efficiency of high power transducers, Ultrasonics 37 (8) (2000) 549–554.
[21] S. Guo, B.C. Khoo, S.L.M. Teo, H.P. Lee, The effect of cavitation bubbles on the removal of juvenile barnacles, Colloids Surf. B: Biointerfaces 109 (2013) 219–227.
[22] B. Lozowicka, M. Jankowska, I. Hrynko, P. Kaczynski, Removal of 16 pesticide residues from strawberries by washing with tap and ozone water, ultrasonic cleaning and boiling, Environ. Monit. Assess. 188 (1) (2016) 1–19.
[23] B. Verhaagen, T. Zanderink, D.F. Rivas, Ultrasonic cleaning of 3D printed objects and cleaning challenge devices, Appl. Acoustics 103 (2016) 172–181.
[24] L. Barnes, D. van der Meulen, B. Orchard, C. Gray, Novel use of an ultrasonic cleaning device for fish reproductive studies, J. Sea Res. 76 (2013) 222–226.
[25] D.D. Nguyen, H.H. Ngo, Y.S. Yoon, S.W. Chang, H.H. Bui, A new approach involving a multi transducer ultrasonic system for cleaning turbine engines' oil filters under practical conditions, Ultrasonics 71 (2016) 256–263.
[26] V. Naddeo, L. Borea, V. Belgiorno, Sonochemical control of fouling formation in membrane ultrafiltration of wastewater: effect of ultrasonic frequency, J. Water Process Eng. 8 (2015) e92–e97.
[27] M. Legay, Y. Allibert, N. Gondrexon, P. Boldo, S. Le Person, Experimental investigations of fouling reduction in an ultrasonically-assisted heat exchanger, Experim. Therm. Fluid Sci. 46 (2013) 111–119.
[28] N.S.M. Yusof, B. Babgi, Y. Alghamdi, M. Aksu, J. Madhavan, M. Ashokkumar, Physical and chemical effects of acoustic cavitation in selected ultrasonic cleaning applications, Ultrason. Sonochem. 29 (2016) 568–576.
[29] R. Jamshidi, Modeling and Numerical Investigation of Acoustic Cavitation with Applications in Sonochemistry, Papierflieger Verlag, 2014.
[30] G.L. Chahine, A. Kapahi, J.-K. Choi, C.-T. Hsiao, Modeling of surface cleaning by cavitation bubble dynamics and collapse, Ultrason. Sonochem. 29 (2016) 528–549.
[31] R. Mettin, P. Koch, W. Lauterborn, D. Krefting, Modeling acoustic cavitation with bubble redistribution, Sixth International Symposium on Cavitation, 2006, pp. 1–5.
[32] J. Lewis, S. Gardner, I. Corp, A 2D finite element analysis of an ultrasonic cleaning vessel: results and comparisons, Int. J. Model. Simul. 27 (2) (2007) 181–185.
[33] V.S. Moholkar, S.P. Sable, A.B. Pandit, Mapping the cavitation intensity in an ultrasonic bath using the acoustic emission, AIChE J. 46 (4) (2000) 684–694.
[34] M. Hodnett, B. Zeqiri, N. Lee, P. Gélat, Report on the feasibility of establishing a reference cavitating medium, NPL Report CMAM 58, National Physical Laboratory, Teddington UK, 2001.
[35] K. Yasui, Y. Iida, T. Tuziuti, T. Kozuka, A. Towata, Strongly interacting bubbles under an ultrasonic horn, Phys. Rev. E 77 (1) (2008) 016609.
[36] M. Ashokkumar, Handbook of Ultrasonics and Sonochemistry, Springer, 2016.
[37] K. Yasui, T. Kozuka, T. Tuziuti, A. Towata, Y. Iida, J. King, P. Macey, FEM calculation of an acoustic field in a sonochemical reactor, Ultrason. Sonochem. 14 (5) (2007) 605–614.
[38] Z. Wei, L.K. Weavers, Combining COMSOL modeling with acoustic pressure maps to design sono-reactors, Ultrason. Sonochem. 31 (2016) 490–498.
[39] L. Zhong, COMSOL multiphysics simulation of ultrasonic energy in cleaning tanks, COMSOL Conference 2014 Boston, (2014).
[40] I. M. G. de C. Esteban-Infantes, Fundamentals of Pipeline Cleaning with Acoustic Cavitation, PhD Thesis, Brunel University London, UK, 2016.
[41] P. Lowe, R. Sanderson, N. Boulgouris, T. Gan, Hybrid active focusing with adaptive dispersion for higher defect sensitivity in guided wave inspection of cylindrical structures, Nondestruct. Test. Eval. 31 (3) (2016) 219–234.
[42] P.S. Lowe, R.M. Sanderson, N.V. Boulgouris, A.G. Haig, W. Balachandran, Inspection of cylindrical structures using the first longitudinal guided wave mode in isolation for higher flaw sensitivity, IEEE Sens. J. 16 (3) (2016) 706–714.
[43] K. Yasui, T. Tuziuti, J. Lee, T. Kozuka, A. Towata, Y. Iida, Numerical simulations of acoustic cavitation noise with the temporal fluctuation in the number of bubbles, Ultrason. Sonochem. 17 (2) (2010) 460–472.